

Low-energy constants and condensates from the τ hadronic spectral functions

Diogo Boito,^a Maarten Golterman,^{b†} Matthias Jamin,^c Kim Maltman,^{d,e}
Santiago Peris^f

^a*Physik Department T31, Technische Universität München, James-Frank-Straße 1
D-85748 Garching, Germany*

^b*Institut de Física d'Altes Energies (IFAE), Universitat Autònoma de Barcelona
E-08193 Bellaterra, Barcelona, Spain*

^c*Institució Catalana de Recerca i Estudis Avançats (ICREA), IFAE
Universitat Autònoma de Barcelona, E-08193 Bellaterra, Barcelona, Spain*

^d*Department of Mathematics and Statistics, York University
Toronto, ON Canada M3J 1P3*

^e*CSSM, University of Adelaide, Adelaide, SA 5005 Australia*

^f*Department of Physics, Universitat Autònoma de Barcelona
E-08193 Bellaterra, Barcelona, Spain*

ABSTRACT

We use results of fits to the OPAL spectral data, obtained from non-strange hadronic τ decays, to evaluate the difference between the vector and axial current correlators, $\Pi_{V-A}(Q^2)$. The behavior of $\Pi_{V-A}(Q^2)$ near euclidean momentum $Q^2 = 0$ is used to determine the effective low-energy constants L_{10}^{eff} and C_{87}^{eff} related to the renormalized low-energy constants L_{10}^r and C_{87}^r in the chiral lagrangian. We also investigate how well two-loop chiral perturbation theory describes $\Pi_{V-A}(Q^2)$ as a function of Q^2 . This is the first determination of L_{10}^{eff} and C_{87}^{eff} to employ a fully self-consistent model for the violations of quark-hadron duality in both the vector and axial channels. We also discuss the values of the coefficients $C_{6,V-A}$ and $C_{8,V-A}$ governing the dimension six and eight contributions to the operator product expansion representation of $\Pi_{V-A}(Q^2)$.

[†] Permanent address: Department of Physics and Astronomy, San Francisco State University, San Francisco, CA 94132, USA

I. INTRODUCTION

Recently, we reanalyzed the OPAL spectral function data for non-strange hadronic τ decays [1], the main aim being a determination of a value for the strong coupling at the τ mass, $\alpha_s(m_\tau^2)$, with a complete error analysis [2, 3]. Among the new elements in this analysis were the use of spectral-function moments with a good perturbative behavior [4], and a complete and self-consistent treatment of non-perturbative effects [3, 5]. This, in turn, requires a quantitative treatment of quark-hadron duality violations (DV) due to the clear presence of hadronic resonances in the spectral function data. The latter was accomplished by employing a model developed in Refs. [6, 7] that we will also use in the present article. While the analysis necessarily relies on this model, we demonstrated that the complete theoretical parametrization of the spectral-function moments including the DV part provides a very good description of the experimental data. We chose to use OPAL data, rather than ALEPH data [8] because of the incompleteness of the data correlations [9] for the latter.

While the central results in Refs. [2, 3] were based on fits to only the vector channel data, we also carried out simultaneous fits to the vector and axial channel data as a consistency check on our results. As a by-product, we thus have a quantitative theoretical description of the vector and axial spectral functions $\rho_V(t)$ and $\rho_A(t)$ from $t = t_{min} \approx 1.3 \text{ GeV}^2$ to $t = \infty$. This lets us evaluate dispersive integrals over $\rho_V(t) - \rho_A(t)$ as a function of euclidean momentum Q quantitatively from the data. (For explicit expressions, see Eqs. (2.1) and (2.10) below.) This, in turn, allows us to extract certain low-energy constants (LECs) appearing in the chiral lagrangian, as well as some of the coefficients appearing in the operator product expansion (OPE), from the low and high Q^2 behavior of $\Pi_{V-A}(Q^2)$, respectively. The determination of these LECs and OPE coefficients is the aim of the present article. As we will explain in detail below, we determine $\Pi_{V-A}(Q^2)$ by summing over experimental data up to $t = t_{\text{switch}}$, and using our fitted spectral functions for $t \in [t_{\text{switch}}, \infty)$, where we will choose $t_{\text{switch}} \in [t_{min}, m_\tau^2]$ (m_τ is the τ mass).

This article is organized as follows. In Sec. II we give a brief overview of the necessary theory, including a rederivation of the Weinberg sum rules beyond the chiral limit tailored to our analysis. In Sec. III we explain our strategy for the numerical evaluation of $\Pi_{V-A}(Q^2)$ and other related functions from the OPAL data. In Sec. IV we present and discuss our results. We include an investigation of a fit of $\Pi_{V-A}(Q^2)$ to chiral perturbation theory (ChPT) to two-loop order. Our conclusions are contained in Sec. V.

II. OVERVIEW OF THEORY

The LECs and OPE condensates this article aims to extract are all related to $\Pi_{V-A}(Q^2)$ defined by¹

$$\Pi_{V-A}(Q^2) = \int_0^\infty dt \frac{\rho_V(t) - \rho_A(t)}{t + Q^2}, \quad (2.1)$$

with Q^2 the euclidean external momentum, and ρ_V (ρ_A) the non-strange $I = 1$ vector (axial) spectral functions summing the angular momentum $J = 1$ and $J = 0$ contributions. Here and in what follows we take, for convenience, ρ_A to be the axial spectral function without the contribution from the pion pole

The difference $\rho_V - \rho_A$ is constrained by the Weinberg sum rules [10]. It is useful to briefly review their derivation, beginning with the second sum rule, because of the subtleties involved at non-zero quark mass. Following Ref. [11], and showing contributions from the pion pole explicitly because it is not contained in $\rho_A(t)$, we write

$$\begin{aligned} \int_0^{s_0} dt w(t) (\rho_V(t) - \rho_A(t)) - 2f_\pi^2 w(m_\pi^2) &= -\frac{1}{2\pi i} \oint_{|z|=s_0} dz w(z) \Pi_{V-A}(z) \\ &= -\frac{1}{2\pi i} \oint_{|z|=s_0} dz w(z) \Pi_{V-A}^{\text{OPE}}(z) - \frac{1}{2\pi i} \oint_{|z|=s_0} dz w(z) \Pi_{V-A}^{\text{DV}}(z), \end{aligned} \quad (2.2)$$

where $w(t)$ is a polynomial in t , and where we split

$$\Pi_{V-A}(z) = \Pi_{V-A}^{\text{OPE}}(z) + \Pi_{V-A}^{\text{DV}}(z) \quad (2.3)$$

into the OPE and duality-violating (DV) parts, following Ref. [6]. The OPE part has the form

$$\Pi_{V-A}^{\text{OPE}}(-Q^2) = \sum_{k=1}^{\infty} \frac{C_{2k,V-A}}{(Q^2)^k}, \quad (2.4)$$

with, for three flavors [11, 12],

$$C_{2,V-A} = -\frac{\alpha_s(\mu^2)}{\pi^3} m_u(\mu^2) m_d(\mu^2) \left(1 - \frac{\alpha_s(\mu^2)}{\pi} \left(\frac{17}{4} \log \frac{Q^2}{\mu^2} + c \right) \right) + \dots, \quad (2.5a)$$

$$C_{4,V-A} = -\frac{8}{3} \frac{\alpha_s}{\pi} f_\pi^2 m_\pi^2 + \dots, \quad (2.5b)$$

where μ is the renormalization scale, $m_{u,d}(\mu^2)$ denote the running up and down quark masses and c is a numerical constant whose value is not required in what follows. In Eq. (2.5b), isospin symmetry has been assumed, and the Gell-Mann–Oakes–Renner relation has been used to express the product of the average light quark mass and quark condensate in terms of f_π and m_π . Contributions from higher-dimensional operators will be neglected. Next, in order to derive the second Weinberg sum rule,

¹ For our conventions, see Ref. [3].

we choose $w(t) = t$. Expressing the DV part of Eq. (2.2) in terms of the DV parts of the vector and axial spectral functions [6],

$$\rho_V^{\text{DV}}(t) - \rho_A^{\text{DV}}(t) = \frac{1}{\pi} \text{Im} \Pi_{V-A}^{\text{DV}}(t) , \quad (2.6)$$

and evaluating the OPE part using Eq. (2.5), Eq. (2.2) can be rewritten as

$$\begin{aligned} & \int_0^{s_0} dt \, t (\rho_V(t) - \rho_A(t)) + \int_{s_0}^{\infty} dt \, t (\rho_V^{\text{DV}}(t) - \rho_A^{\text{DV}}(t)) \\ &= 2f_\pi^2 m_\pi^2 \left(1 + \frac{4}{3} \frac{\alpha_s(s_0)}{\pi} \right) + \frac{17}{4\pi^2} \left(\frac{\alpha_s(s_0)}{\pi} \right)^2 m_u(s_0) m_d(s_0) s_0 , \end{aligned} \quad (2.7)$$

where we set $\mu^2 = s_0$. This is the version of the second Weinberg sum rule we will employ. A similar derivation, choosing $w(t) = 1$, leads to the first Weinberg sum rule,

$$\int_0^{s_0} dt (\rho_V(t) - \rho_A(t)) + \int_{s_0}^{\infty} dt (\rho_V^{\text{DV}}(t) - \rho_A^{\text{DV}}(t)) = 2f_\pi^2 , \quad (2.8)$$

where we already dropped the correction coming from the OPE contributions to the right-hand side of Eq. (2.2), as these are numerically tiny for the s_0 of interest to us. Our conventions are such that $f_\pi = 92.21(14)$ MeV.

The effective LECs L_{10}^{eff} and C_{87}^{eff} are defined from the expansion of $\Pi_{V-A}(Q^2)$ around $Q^2 = 0$ [13–15]:

$$\Pi_{V-A}(Q^2) = -8L_{10}^{\text{eff}} - 16C_{87}^{\text{eff}} Q^2 + O(Q^4) , \quad (2.9)$$

while the OPE condensates $C_{6,V-A}$ and $C_{8,V-A}$ are defined from the high- Q^2 expansion (2.4).

We will also use functions $\Pi_{V-A}^{(w)}$ involving additional polynomial weight factors $w(x)$, defined by

$$\Pi_{V-A}^{(w)}(Q^2) = \int_0^{\infty} dt \, w(t/s_0) \frac{\rho_V(t) - \rho_A(t)}{t + Q^2} . \quad (2.10)$$

The weights we will consider are

$$w_k(x) = (1 - x)^k , \quad k = 1, 2 . \quad (2.11)$$

Using the Weinberg sum rules Eqs. (2.7) and (2.8), one finds

$$\begin{aligned} -8L_{10}^{\text{eff}} &= \Pi_{V-A}(0) = \Pi_{V-A}^{(w_1)}(0) + \frac{2f_\pi^2}{s_0} \\ &= \Pi_{V-A}^{(w_2)}(0) + \frac{4f_\pi^2}{s_0} \left[1 - \frac{17}{16\pi^2} \left(\frac{\alpha_s(s_0)}{\pi} \right)^2 \frac{m_u(s_0) m_d(s_0)}{f_\pi^2} - \frac{m_\pi^2}{2s_0} \left(1 + \frac{4}{3} \frac{\alpha_s(s_0)}{\pi} \right) \right] , \end{aligned} \quad (2.12)$$

yielding alternative ways to evaluate L_{10}^{eff} . Similar equations can be derived for C_{87}^{eff} . In these equations, we assumed that $\Pi_{V-A}^{(w)}(Q^2)$ can be written as in Eq. (2.10), using the experimental spectral functions for $t \leq s_0$, and the approximation

$$\rho_V(t) - \rho_A(t) \approx \rho_V^{\text{DV}}(t) - \rho_A^{\text{DV}}(t) , \quad t \geq s_0 , \quad (2.13)$$

above s_0 , *cf.* Eq. (2.7). This approximation involves the assumption that OPE contributions in principle present in the theoretical representation of $\rho_V - \rho_A$ are numerically tiny and can be safely neglected. We can test this assumption by evaluating the OPE corrections in Eq. (2.12), which in that equation appear as the terms depending on $\alpha_s(s_0)$. Setting $s_0 = m_\tau^2$ and using $\alpha_s(m_\tau^2)/\pi \approx 0.1$ and $m_{u,d}(m_\tau^2) < 10$ MeV, we find that the second term inside the square brackets is at most of order 10^{-5} . The term proportional to $m_\pi^2 \alpha_s(s_0)/s_0$ inside the square brackets is of order 4×10^{-4} at the τ mass. For values of s_0 down to 1.5 GeV^2 it will be larger, but even an order of magnitude will not affect our results below.² In fact, the contribution from the term $2f_\pi^2 m_\pi^2/s_0^2$ to L_{10}^{eff} itself is very small, about 2×10^{-5} . For our purposes, the dimension two and four OPE corrections to the approximation (2.13) turn out to be completely negligible, and it will be justified to drop the terms in Eq. (2.12) containing factors of $\alpha_s(s_0)$ in Sec. IV below.³

For the DV part of the vector and axial spectral functions, we will use the parametrization

$$\rho_{V/A}^{\text{DV}}(t) = e^{-\delta_{V/A} - \gamma_{V/A} t} \sin(\alpha_{V/A} + \beta_{V/A} t) , \quad (2.14)$$

where $\alpha_{V/A}$, $\beta_{V/A}$, $\gamma_{V/A}$, and $\delta_{V/A}$ are eight free DV parameters, which are fitted to moments of the experimental spectral functions. For a detailed discussion and history of this parametrization, see Refs. [6, 7, 17].

III. STRATEGY AND DATA

We will evaluate $\Pi_{V-A}(Q^2)$ and $\Pi_{V-A}^{(w_k)}(Q^2)$ using OPAL experimental data [1] for the spectral functions $\rho_V(t)$ and $\rho_A(t)$ for $t \leq s_0 = t_{\text{switch}}$, and approximating the difference $\rho_V(t) - \rho_A(t)$ by Eq. (2.13) for $t \geq s_0 = t_{\text{switch}}$, with values for the DV parameters from our previous fits to the data. We used adjusted OPAL data, updated to reflect current values of exclusive mode hadronic τ -decay branching fractions, as described in Ref. [2]. We will choose t_{switch} to be the upper end of OPAL bin N , obtaining

$$\begin{aligned} \Pi_{V-A}^{(w)}(Q^2) = & \sum_{i=1}^N \Delta t w(t[i]/t_{\text{switch}}) \frac{\rho_V(t[i]) - \rho_A(t[i])}{t[i] + Q^2} \\ & + \int_{t_{\text{switch}}}^{\infty} dt w(t/t_{\text{switch}}) \frac{\rho_V^{\text{DV}}(t) - \rho_A^{\text{DV}}(t)}{t + Q^2} . \end{aligned} \quad (3.1)$$

Here $\Delta t = 0.032 \text{ GeV}^2$ is the OPAL bin width and $t[i] = (i - 1/2)\Delta t$ is the midpoint value of the i th bin; $t_{\text{switch}} = t[N] + \Delta t/2 = N\Delta t$. $\Pi_{V-A}(Q^2)$ is obtained by setting the polynomial weight $w = 1$.

² We will therefore also not worry about higher-order corrections in α_s omitted from Eqs. (2.7) and (2.12) above, even though typically the perturbative expansions of the coefficients $C_{2k,V-A}$ converge slowly for the $J = 0$ component.

³ A less quantitative version of this argument appeared in Ref. [16].

The simplest fits from which the DV parameters were obtained were fits to the separate vector and axial versions of Eq. (2.2) with $w(t) = 1$, using OPAL data to evaluate the moments

$$I_{V/A}(s_0) = \int_0^{s_0} dt \rho_{V/A}(t) \quad (3.2)$$

through a Riemann-sum approximation like the one shown in Eq. (3.1), and varying s_0 between a given s_{min} and m_τ^2 . For $w(t) = 1$, all OPE contributions except the $D = 0$ perturbative ones are negligible, and a fit to $I_{V/A}(s_0)$ thus yields α_s and the DV parameters of the channel in question.⁴ The value of s_{min} was determined by requiring a good quality match between the experimental $I_{V/A}(s_0)$ and fitted theoretical representations, and stability of the fit parameters with respect to variation of s_{min} . In this article, we will always choose $t_{switch} = s_{min}$.⁵ Our central results were obtained with the choice $s_{min} = 1.504 \text{ GeV}^2$.⁶ We have also used the more elaborate moments with weights $1 - (t/s_0)^2$ and the “ τ kinematic weight” $(1 - t/s_0)^2(1 + 2t/s_0)$ inserted into Eq. (3.2); the perturbative part of all moments was evaluated using both fixed-order (FOPT) and contour-improved (CIPT) [18] perturbation theory. The non-trivially weighted moments also give access to the OPE coefficients $C_{6,V/A}$ and $C_{8,V/A}$. Both pure vector and combined vector and axial channel fits were investigated. For a detailed account of all these fits, we refer to Refs. [2, 3]. The fit results employed here are always those from Ref. [2], unless otherwise noted.

We have fully propagated all errors and correlations in the results we will report on below. In particular, the DV parameter values used in Eq. (3.1) are correlated with the data, and we have computed these correlations using the linear error propagation method summarized in the appendix of Ref. [3] (see, in particular, Eq. (A.4) of that reference, which can be used to express the parameter-data covariances in terms of the data covariance matrix).

IV. RESULTS

We will begin with presenting the results for L_{10}^{eff} and C_{87}^{eff} as defined by Eq. (2.9), using Eq. (2.12) as well. After that, we will check the convergence of chiral perturbation theory by fitting the Q^2 dependence to the two-loop expressions for Π_{V-A} calculated in Ref. [14]. Then, in Sec. IV C, we will revisit the dimension 6 and 8 OPE coefficients.

A. L_{10}^{eff} and C_{87}^{eff}

Table 1 shows results relevant for L_{10}^{eff} . This LEC can be directly obtained from the second column using Eq. (2.9), or from the fourth or sixth column using Eq. (2.12). The DV parts of these integrals, corresponding to the second term on the right-hand

⁴ α_s was enforced to be equal in the two channels.

⁵ We have explored taking $t_{switch} > s_{min}$, and find that this leads to results fully consistent with the choice $t_{switch} = s_{min}$ and no reduction in errors.

⁶ This value corresponds to the upper end of OPAL bin 47.

s_{min}	$\Pi_{V-A}(0)$	$\Pi_{V-A}^{DV}(0)$	$\Pi_{V-A}^{(w_1)}(0)$	$\Pi_{V-A}^{(w_1)DV}(0)$	$\Pi_{V-A}^{(w_2)}(0)$	$\Pi_{V-A}^{(w_2)DV}(0)$
1.408	0.0522(10)	-0.0039	0.04019(88)	-0.00042	0.02738(72)	0.00028
1.504	0.0522(11)	-0.0019	0.04083(90)	-0.00071	0.02915(72)	0.00033
1.600	0.0523(11)	-0.0001	0.04081(90)	-0.00066	0.02916(72)	0.00013
1.504	0.0522(11)	-0.0019	0.04081(91)	-0.00072	0.02916(72)	0.00034

TABLE 1: Values of Π_{V-A} , $\Pi_{V-A}^{(w_1)}$, and $\Pi_{V-A}^{(w_2)}$ at $Q^2 = 0$. We always take the switch point between data and the duality-violating part of the spectral function at $t_{\text{switch}} = s_{min}$ (values for s_{min} are in GeV^2). The superscript DV indicates the contribution from the second term on the right-hand side of Eq. (3.1). Duality violation parameters are from the fits of Ref. [2], Table 3. Results from fits using FOPT are shown above the double line, those from CIPT below.

side of Eq. (3.1), are shown in the third, fifth and seventh columns. Note that the (absolute) errors become smaller with increasing k in Eq. (2.11), *i.e.*, with more pinching at $s_{min} = t_{\text{switch}}$. We also note that the results are essentially independent of s_{min} , and whether one chooses the FOPT or CIPT scheme for the evaluation of the truncated perturbative series. This is a consequence of the fact that the integrals are almost completely determined by the data part, *i.e.*, the sum on the first line of Eq. (3.1), as can be seen from the always small contribution from the DV part of the integrals. We will henceforth use the FOPT results at $s_{min} = 1.504 \text{ GeV}^2$.

From Eq. (2.9) we find

$$L_{10}^{\text{eff}} = (-6.52 \pm 0.14) \times 10^{-3} \quad (\text{from } \Pi_{V-A}(0)) . \quad (4.1)$$

Using Eq. (2.12), one may also compute L_{10}^{eff} from the other values shown in Table 1; the results are always consistent within errors. In fact, using $\Pi_{V-A}^{(w_{1,2})}$ and Eq. (2.12), we obtain the somewhat more precise values:

$$\begin{aligned} L_{10}^{\text{eff}} &= (-6.52 \pm 0.11) \times 10^{-3} \quad (\text{from } \Pi_{V-A}^{(w_1)}(0)) , \\ &= (-6.45 \pm 0.09) \times 10^{-3} \quad (\text{from } \Pi_{V-A}^{(w_2)}(0)) . \end{aligned} \quad (4.2)$$

These values are in good agreement with the value found recently in Ref. [19], except that our best error is twice as large. There are (at least) two reasons for this difference in errors, both of which point to the error in Ref. [19] being underestimated.⁷ First, Refs. [16, 19] used a DV *ansatz* of the functional form shown in Eq. (2.14) for the *difference* $\rho_V^{\text{DV}} - \rho_A^{\text{DV}}$, instead of using this form for each channel separately. That implies that Refs. [16, 19] used only four parameters to describe duality violations in $V - A$, whereas we use eight. The simplified four-parameter form assumed in

⁷ For more comments on the comparison with Ref. [19], we refer to the Conclusion.

s_{min}	$\Pi'_{V-A}(0)$	$\Pi'^{DV}_{V-A}(0)$
1.408	-0.1356(47)	0.0029
1.504	-0.1355(47)	0.0016
1.600	-0.1356(47)	0.0004
1.504	-0.1355(47)	0.0016

TABLE 2: Values of Π'_{V-A} at $Q^2 = 0$ obtained by differentiating Eq. (2.1) with respect to Q^2 . We always take the switch point between data and the duality-violating part of the spectral function at $t_{\text{switch}} = s_{min}$. The superscript DV indicates the contribution from the second term on the right-hand side of Eq. (3.1). Duality violation parameters are from the fits of Ref. [2], Table 3. Results from fits using FOPT are shown above the double line, those from CIPT below.

Refs. [16, 19] would be valid if it happened, for some reason, that $\gamma_V = \gamma_A$ and $\beta_V = \beta_A$. Since we find very different values for γ_V and γ_A in our fits to both the OPAL data [2] and the ALEPH data [20], this condition is, however, not satisfied. The theoretical systematic error associated with the breakdown of this assumption is, of course, not included in the error estimates of Refs. [16, 19]. These comments remain relevant even if an *ansatz* of the form (2.14) gives a reasonable description of the difference $\rho_V(t) - \rho_A(t)$ for large enough t : a model description of duality violations is only acceptable if it describes the resonance physics at higher energies in both the vector and axial channels individually. The second reason for our larger error is that Ref. [19] used the formally more precise, but in practice incomplete ALEPH data [9]. If ALEPH data with corrected correlation matrices were to become available, we anticipate that errors would be reduced relative to those obtained using the OPAL data for our fits as well.

Values for the derivative of $\Pi_{V-A}(Q^2)$ with respect to Q^2 at $Q^2 = 0$ are shown in Table 2. As one would expect, the results show the same robustness with respect to the various fits of Ref. [2] as those in Table 1. Using Eq. (3.1), we find

$$C_{87}^{\text{eff}} = (8.47 \pm 0.29) \times 10^{-3} \text{ GeV}^{-2} . \quad (4.3)$$

This value again agrees with that found in Ref. [19], but our error is again about twice as large. Using the cubic doubly-pinched weight of Ref. [5] in Eq. (2.10) as was done in Ref. [19] does not lead to a smaller error in our case. The same comments about the reasons for our larger error as discussed above for L_{10}^{eff} apply here as well.

We have repeated the analysis presented here using fit values for the DV parameters reported in Table 5 of Ref. [2], again taking all correlations into account. The results for L_{10}^{eff} and C_{87}^{eff} are virtually identical to those reported above.

B. Connection to chiral perturbation theory

The LECs L_{10}^{eff} and C_{87}^{eff} , which are defined by the values at $Q^2 = 0$ of $\Pi_{V-A}(Q^2)$ and its derivative (cf. Eq. (2.9)), are connected to LECs in the order- p^6 chiral lagrangian through the relations [15]

$$\Pi_{V-A}(0) = -8L_{10}^{\text{eff}} \quad (4.4a)$$

$$\begin{aligned} &= -8L_{10}^r(\mu) \left(1 - 4(2\mu_\pi + \mu_K) \right) + 16(2\mu_\pi + \mu_K)L_9^r(\mu) \\ &\quad - \frac{1}{16\pi^2} \left(1 - \log \frac{\mu^2}{m_\pi^2} + \frac{1}{3} \log \frac{m_K^2}{m_\pi^2} \right) - 8G_{2L}(\mu, 0) \\ &\quad - 32m_\pi^2 (C_{61}^r(\mu) - C_{12}^r(\mu) - C_{80}^r(\mu)) \\ &\quad - 32(2m_K^2 + m_\pi^2) (C_{62}^r(\mu) - C_{13}^r(\mu) - C_{81}^r(\mu)) , \\ -\Pi'_{V-A}(0) &= 16C_{87}^{\text{eff}} \quad (4.4b) \end{aligned}$$

$$\begin{aligned} &= 16C_{87}^r(\mu) + \frac{1}{480\pi^2} \left(\frac{1}{m_\pi^2} + \frac{2}{m_K^2} \right) - 8 \frac{\partial G_{2L}(\mu, s)}{\partial s} \Big|_{s=0} \\ &\quad - \frac{1}{4\pi^2 f_\pi^2} \left(1 - \log \frac{\mu^2}{m_\pi^2} + \frac{1}{3} \log \frac{m_K^2}{m_\pi^2} \right) L_9^r(\mu) , \\ \mu_P &= \frac{m_P^2}{32\pi^2 f_\pi^2} \log \frac{m_P^2}{\mu^2} . \quad (4.4c) \end{aligned}$$

Here the superscript r denotes the values of LECs renormalized at scale μ , which below we will take to be $\mu = 0.77$ GeV.

The complete order- p^6 ChPT expression for $\Pi_{V-A}(Q^2)$ can be written as a function of Q^2 in terms of the renormalized LECs $L_{9,10}^r$ and $C_{12,13,61,62,80,81,87}^r$ using the results of Ref. [14].⁸ Choosing $\mu = 0.77$ GeV, and using $m_\pi = 139.570$ MeV and $m_K = 495.65$ MeV, the Q^2 dependence of $\Pi_{V-A}(Q^2)$ in chiral perturbation theory to order p^6 takes the form

$$\begin{aligned} \Pi_{V-A}(Q^2) &= -12.165L_{10}^r - 32m_\pi^2 (C_{61}^r - C_{12}^r - C_{80}^r) \quad (4.5) \\ &\quad - 32(2m_K^2 + m_\pi^2) (C_{62}^r - C_{13}^r - C_{81}^r) - 16C_{87}^r Q^2 + R(Q^2; L_9^r) , \end{aligned}$$

where $R(Q^2; L_9^r)$ is a fully known non-analytic function in Q^2 coming from one- and two-loop contributions in ChPT, including one-loop contributions with a vertex containing L_9^r . Note that $R(Q^2; L_9^r)$ also depends on the scale μ , even though we have not explicitly indicated any such dependence in Eq. (4.5), because we evaluated the numerical value of the coefficient of L_{10}^r at $\mu = 0.77$ GeV. This implies that both $R(Q^2; L_9^r)$ and all LECs appearing in this equation are to be evaluated at this value of μ . At $Q^2 = 0$, Eq. (4.5) yields Eq. (4.4), through the relation (2.9).

If we fit $\Pi_{V-A}(Q^2)$ to this order- p^6 expression, we can explore the range in Q^2 for which order- p^6 ChPT is a valid approximation. Note that the order- p^6 expression is not linear in Q^2 , even though Eq. (2.9), which one obtains upon re-expanding the

⁸ We do not quote those results here because of their length.

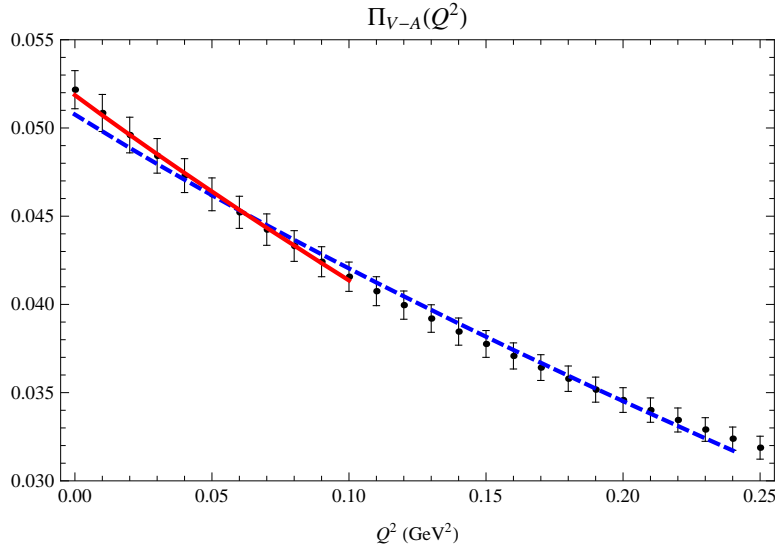


FIG. 1: ChPT fits at order p^6 to $\Pi_{V-A}(Q^2)$. The blue (dashed) curve includes Q^2 values up to 0.24 GeV^2 ; the red (continuous) curve includes Q^2 values up to 0.10 GeV^2 .

order- p^6 ChPT expression for $Q^2 < 4m_\pi^2$, is linear in Q^2 .⁹ With m_π and m_K fixed to their physical values, the data can, of course, not be used to separate the Q^2 -independent part of Eq. (4.5) into its individual order- p^4 and order- p^6 components without additional input. Such input might be obtained in the future from lattice studies employing a range of light quark masses.

We have carried out a fit to Eq. (4.5) in terms of L_{10}^r and C_{87}^r , using given values for all the other LECs on the right-hand side of Eq. (4.4). Specifically, we chose the central values $L_9^r(\mu) = 0.00593$ [23], $4m_\pi^2(C_{61}^r(\mu) - C_{12}^r(\mu) - C_{80}^r(\mu)) = -0.000067$ and $C_{62}^r(\mu) - C_{13}^r(\mu) - C_{81}^r(\mu) = 0$ [15] at $\mu = 0.77 \text{ GeV}$,¹⁰ for which Eq. (4.4) becomes

$$L_{10}^{\text{eff}} = 1.521L_{10}^r(\mu = 0.77 \text{ GeV}) - 0.000288, \quad (4.6a)$$

$$C_{87}^{\text{eff}} = C_{87}^r(\mu = 0.77 \text{ GeV}) + 0.00328 \text{ GeV}^{-2}, \quad (4.6b)$$

where we also used $m_\eta = 547.853 \text{ MeV}$ (the latter is needed for the evaluation of the loop contributions to the constants in these equations).

Fits to ChPT at order p^6 are shown in Fig. 1. The blue (dashed) curve shows a fit with a maximum Q^2 value $Q_{\text{max}}^2 = 0.24 \text{ GeV}^2$, while the red (continuous) curve shows a fit with $Q_{\text{max}}^2 = 0.10 \text{ GeV}^2$. The fits were performed using points beginning at $Q^2 = 0$ and spaced by 0.01 GeV^2 . These data, computed from Eq. (3.1), are strongly correlated, and not amenable to a standard χ^2 fit, forcing us to perform a fit with diagonal inverse-squared-error weighting.¹¹ The full data correlations are then

⁹ The threshold in the dispersive integral for $\Pi_{V-A}(Q^2)$ is $4m_\pi^2$, and not m_π^2 , since the π pole contribution was subtracted in defining $\rho_A(t)$.

¹⁰ Errors on these values are only needed if one wishes to convert values for L_{10}^{eff} and C_{87}^{eff} into values for L_{10}^r and C_{87}^r . For such an analysis, we refer to Ref. [15].

¹¹ Thinning out the data does not help.

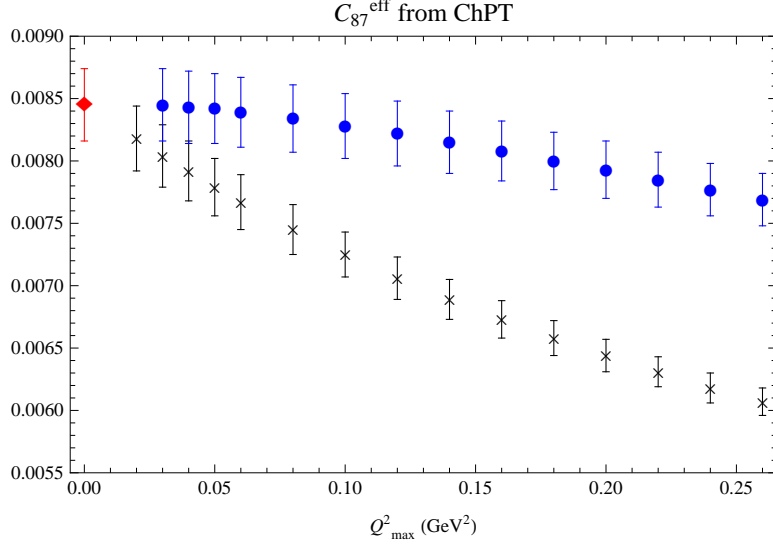


FIG. 2: Black points (crosses) show values of C_{87}^{eff} obtained from the ChPT fits as a function of Q_{max}^2 , the maximum Q^2 value used in the fit. The red point (diamond) at $Q_{max}^2 = 0$ is the value of Eq. (4.3), for comparison. The blue points (filled circles) have been obtained from a fit to Eq. (4.5) with a term proportional to Q^4 added to it; see text for further details.

taken into account in the quoted errors using the technique described in the appendix of Ref. [3].

Clearly, the blue curve does not provide a good fit, while the red curve does. We conclude that ChPT at this order gives a good match to $\Pi_{V-A}(Q^2)$ up to $Q \approx 300$ MeV, which is about twice the pion mass. The ChPT fits are virtually linear, suggesting consistency with the extraction of L_{10}^{eff} and C_{87}^{eff} from Eq. (2.9). From the ChPT fit corresponding to the red curve in Fig. 1, we obtain the values $L_{10}^r = -4.08(9) \times 10^{-3}$ and $C_{87}^r = 3.97(18) \times 10^{-3} \text{ GeV}^{-2}$, which correspond to

$$\begin{aligned} L_{10}^{\text{eff}} &= (-6.49 \pm 0.14) \times 10^{-3}, \\ C_{87}^{\text{eff}} &= (7.25 \pm 0.18) \times 10^{-3} \text{ GeV}^{-2}. \end{aligned} \quad (4.7)$$

The value for L_{10}^{eff} is completely consistent with Eqs. (4.1) and (4.2), but this is not the case for the value of C_{87}^{eff} , which is not consistent within errors with Eq. (4.3). The reason for this is that the value in Eq. (4.3) was obtained from the behavior of $\Pi_{V-A}(Q^2)$ near $Q^2 = 0$, while the value in Eq. (4.7) was obtained by a fit of $\Pi_{V-A}(Q^2)$ over the range $0 \leq Q^2 \leq Q_{max}^2 = 0.1 \text{ GeV}^2$. Values for C_{87}^{eff} obtained by varying Q_{max}^2 are shown as the black points (crosses) in Fig. 2. This figure shows that ChPT to order p^6 does a reasonable job in describing $\Pi_{V-A}(Q^2)$, but clearly order- p^8 effects, not included in the chiral fits, are present in the data. In contrast, the value of L_{10}^{eff} is barely affected by varying Q_{max}^2 ; it varies by less than the errors quoted in Eq. (4.2) over the range shown in Fig. 2.

The presence of order- p^8 effects can be checked by redoing the ChPT fits, but now using Eq. (4.5) with an extra term $+DQ^4$ added. This is of course a phenomenological

fit, because the order- p^8 structure is more complicated than just such a simple term. But Fig. 1 shows that the deteriorating quality of the fits with larger values of Q_{max}^2 is due to some curvature showing up in $\Pi_{V-A}(Q^2)$ at larger Q^2 , and we expect this extra term to capture this curvature reasonably well. We show the results for C_{87}^{eff} as a function of Q_{max}^2 with this new term included in the fit as the blue points (filled circles) in Fig. 2. Indeed, the values for C_{87}^{eff} become much less sensitive to Q_{max}^2 , with values consistent with Eq. (4.3) over a much larger range. We also find that L_{10}^{eff} does not change significantly as a consequence of this exercise: instead of the value in Eq. (4.7) we now obtain $L_{10}^{\text{eff}} = (-6.52 \pm 0.14) \times 10^{-3}$. The phenomenological coefficient D varies between 0.2 and 0.1 over the interval shown in the figure.

The lesson of this exploration is that any values of L_{10}^r and C_{87}^r obtained from L_{10}^{eff} and C_{87}^{eff} using (as in Ref. [15]) the order- p^6 ChPT relations of Eq. (4.4) must be treated with some care. While terms beyond order- p^6 in the chiral counting associated with higher powers of Q^2 can be removed by taking Q^2 to zero, those associated with higher powers of the quark masses are fixed by the non-zero, physical meson masses and cannot be removed. Such contributions are present in the relations between L_{10}^{eff} and L_{10}^r and C_{87}^{eff} and C_{87}^r to arbitrarily high chiral order. The variation in the fitted value of C_{87}^r with Q_{max}^2 (the source of the variation of C_{87}^{eff} displayed in Fig. 2, cf. Eq. (4.6b)) indicates non-trivial Q^2 -dependent contributions of order- p^8 and beyond, raising the possibility of analogous mass-dependent, Q^2 -independent order- p^8 (and beyond) contributions as well.

The impact of such order- p^8 (and higher) contributions will be more significant for the relation between C_{87}^{eff} and C_{87}^r than for that between L_{10}^{eff} and L_{10}^r since in the former case the missing order- p^8 terms are only one chiral order higher than the LEC of interest, C_{87}^r , whereas in the latter case the missing terms begin two chiral orders higher than L_{10}^r . Even so, the order- p^8 and higher contributions need not be completely negligible for L_{10}^r . In fact, ignoring the contributions of the order- p^6 LECs $C_{12,13,61,62,80,81}$ to the relation between L_{10}^{eff} and L_{10}^r , the effects of the mass-dependent order- p^6 terms are significant, changing the coefficient of L_{10}^r from 1 at order- p^4 to 1.521 at order- p^6 in Eq. (4.6a), and altering the best fit results for L_{10}^r by about 30% between order- p^4 and order- p^6 . A further shift in L_{10}^r by about $0.3^2 \approx 10\%$ due to order- p^8 effects would thus not be unexpected. Similarly, a difference of about 30% between the order- p^6 and order- p^8 values for C_{87}^r would not be surprising.

In conclusion, if estimates for L_{10}^r and C_{87}^r obtained from L_{10}^{eff} and C_{87}^{eff} are used in the computation of some other physical quantity, propagating the error quoted in Eqs. (4.2) and (4.3) would not include additional systematic errors due to the omission of order- p^8 terms in ChPT.

C. $V - A$ condensates

In this subsection, we consider the values of the OPE coefficients $C_{6,V-A}$ and $C_{8,V-A}$, defined in Eq. (2.4). In Ref. [2] we presented fit results for $C_{6,V/A}$ and $C_{8,V/A}$ obtained using sum rules involving weights up to degree three, from which it is straightforward to obtain $C_{6,V-A}$ and $C_{8,V-A}$. From the fits at $s_{min} = 1.504 \text{ GeV}^2$,

and including all correlations, we find the values

$$\begin{aligned} C_{6,V-A} &= (-10.5 \pm 2.8) \times 10^{-3} \text{ GeV}^6 & (\text{FOPT}) , \\ &= (-11.3 \pm 2.4) \times 10^{-3} \text{ GeV}^6 & (\text{CIPT}) , \end{aligned} \quad (4.8a)$$

$$\begin{aligned} C_{8,V-A} &= (14 \pm 7) \times 10^{-3} \text{ GeV}^8 & (\text{FOPT}) , \\ &= (16 \pm 6) \times 10^{-3} \text{ GeV}^8 & (\text{CIPT}) . \end{aligned} \quad (4.8b)$$

Changes as a function of varying s_{\min} are small compared to the errors shown in Eq. (4.8).

It is interesting to compare these values with those we would obtain from the original OPAL data, to which no correction reflecting modern values for the τ hadronic branching fractions have been applied. In this case, we find, using the fits reported in Table 5 of Ref. [3]:

$$\begin{aligned} C_{6,V-A} &= (-3 \pm 4) \times 10^{-3} \text{ GeV}^6 & (\text{FOPT}) , \\ &= (-4 \pm 4) \times 10^{-3} \text{ GeV}^6 & (\text{CIPT}) , \end{aligned} \quad (4.9a)$$

$$\begin{aligned} C_{8,V-A} &= (-3 \pm 12) \times 10^{-3} \text{ GeV}^8 & (\text{FOPT}) , \\ &= (0 \pm 12) \times 10^{-3} \text{ GeV}^8 & (\text{CIPT}) . \end{aligned} \quad (4.9b)$$

The results for $C_{6,V-A}$ and $C_{8,V-A}$ are barely consistent between the updated and original OPAL data. The relatively large differences between the “updated” and “original” data are not a big surprise: these OPE coefficients parametrize the most subleading part of the fits carried out in Refs. [2, 3]. Moreover, it was found that the fits reported in Table 5 of Ref. [2], while consistent with simpler fits, are at the “statistical edge” of what can be extracted from the OPAL data.

One can avoid using the fits of Table 5 of Ref. [2] by employing the sum rule (2.2) with a judicious choice of the weights $w(t)$. As we have seen, $\rho_V(t) - \rho_A(t)$ can be obtained from the simpler fits reported in Table 3 of Ref. [2]. An obvious possibility is to choose $w(t) = t^2$ or $w(t) = t^3$, for which the right-hand side of Eq. (2.2) immediately yields $C_{6,V-A}$, respectively, $-C_{8,V-A}$. We find results consistent with those reported in Eq. (4.8), with comparable errors.

However, using the moments of Ref. [5], which involve a double-pinching factor $(t - t_{\text{switch}})^2$, we can do better.¹² Choosing $w(t) = (t - t_{\text{switch}})^2$ or $w(t) = (t - t_{\text{switch}})^2(t + 2t_{\text{switch}})$, Eq. (2.2) implies

$$\begin{aligned} C_{6,V-A} &= \sum_{i=1}^N \Delta t (t[i] - t_{\text{switch}})^2 (\rho_V(t[i]) - \rho_A(t[i])) - 2f_\pi^2(m_\pi^2 - t_{\text{switch}})^2 \\ &\quad + \int_{t_{\text{switch}}}^{\infty} dt (t - t_{\text{switch}})^2 (\rho_V^{\text{DV}}(t) - \rho_A^{\text{DV}}(t)) , \end{aligned} \quad (4.10a)$$

$$\begin{aligned} C_{8,V-A} &= - \sum_{i=1}^N \Delta t (t[i] - t_{\text{switch}})^2(t[i] + 2t_{\text{switch}}) (\rho_V(t[i]) - \rho_A(t[i])) \\ &\quad + 2f_\pi^2(m_\pi^2 - t_{\text{switch}})^2(m_\pi^2 + 2t_{\text{switch}}) \\ &\quad - \int_{t_{\text{switch}}}^{\infty} dt (t - t_{\text{switch}})^2(t + 2t_{\text{switch}}) (\rho_V^{\text{DV}}(t) - \rho_A^{\text{DV}}(t)) . \end{aligned} \quad (4.10b)$$

¹² This method was also employed in Ref. [19].

s_{min}	$10^3 C_{6,V-A}$	$10^3 C_{6,V-A}^{DV}$	$10^3 C_{8,V-A}$	$10^3 C_{8,V-A}^{DV}$
1.408	-7.3(5)	0.8	8(2)	-3
1.504	-6.2(9)	1.2	3(4)	-5
1.600	-6.4(8)	0.3	4(4)	-1
1.504	-6.2(9)	1.2	3(4)	-5

TABLE 3: $C_{6,V-A}$ (in GeV^6) and $C_{8,V-A}$ (in GeV^8) from Eq. (4.10). The superscript DV indicates the part coming from the DV integrals in Eq. (4.10). Duality violation parameters are from the fits of Ref. [2], Table 3. Results from fits using FOPT are shown above the double line, those from CIPT below.

In these expressions, the sums over bins, as well as the pion-pole terms, are obtained from data, the latter with negligible errors.¹³ These sum rules have two advantages: (1) they suppress the data at higher t , which have larger errors, and (2) they suppress the contribution from the DV-integral terms [5, 19], replacing these contributions, in effect, by the pion-pole terms, which are known with great precision.

We present the results in Table 3. The DV parts are significantly smaller than those we would obtain with $w(t) = t^2$ or $w(t) = t^3$, especially for $C_{6,V-A}$, but also for $C_{8,V-A}$. And indeed, errors are also significantly smaller than those of Eq. (4.8), as we expected. We note, however, that there is some discrepancy between the values of Table 3 and Eq. (4.8). The results of Table 3 are based on results from simpler and more stable fits reported in Table 3 of Ref. [2].¹⁴ Therefore, we take as our central results for $C_{6,V-A}$ and $C_{8,V-A}$ the values from Table 3 above,

$$\begin{aligned} C_{6,V-A} &= (-6.6 \pm 1.1) \times 10^{-3} \text{ GeV}^6, \\ C_{8,V-A} &= (5 \pm 5) \times 10^{-3} \text{ GeV}^8, \end{aligned} \quad (4.11)$$

where the central values are the averages of the values in Table 3, and the errors have been obtained by adding the fitting error at $s_{min} = 1.504 \text{ GeV}^2$ and the variation as a function of s_{min} in quadrature.

In Fig. 3 we compare our results with other results in the literature. Updating the OPAL data without including DVs in the analysis causes the central values of the OPAL-based results of Ref. [22] to shift from $C_{6,V-A} = -5.4 \times 10^{-3} \text{ GeV}^6$, $C_{8,V-A} = -1.4 \times 10^{-3} \text{ GeV}^8$ to $C_{6,V-A} = -5.0 \times 10^{-3} \text{ GeV}^6$ and $C_{8,V-A} = -3.4 \times 10^{-3} \text{ GeV}^8$. A comparison of the latter set to the results of the present analysis then shows directly the impact of the inclusion of DVs.¹⁵

¹³ Order- α_s corrections from dimension two and four terms in the OPE are again completely negligible.

¹⁴ For an extensive discussion of the quality of these fits, we refer to Ref. [2].

¹⁵ The reader should note that, for the s_0 employed in the fits of Ref. [22], integrated DVs have the opposite sign to those shown in Table 3.

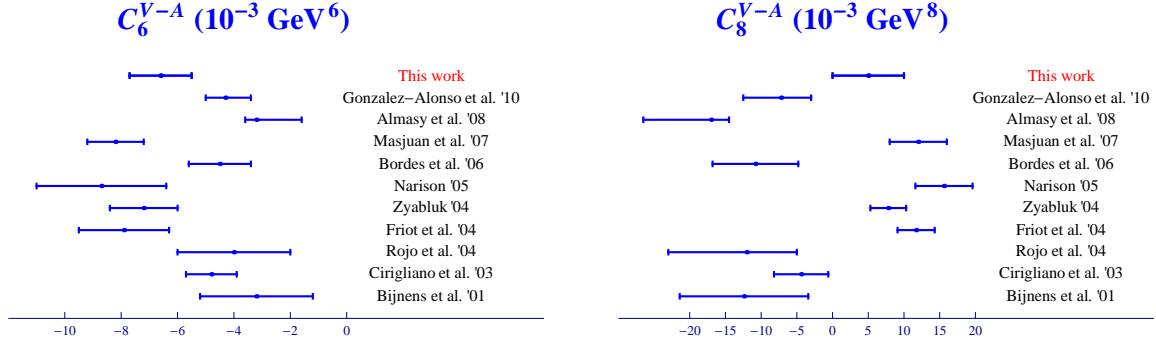


FIG. 3: Comparison with other recent values [19, 21, 22] for $C_{6,V-A}$ (left panel) and $C_{8,V-A}$ (right panel).

We note in particular that our values do not agree with those found in Ref. [19]. While our discussion above indicates that the determination of $C_{6,V-A}$ and $C_{8,V-A}$ is limited by the quality of the data, we also recall that Ref. [19] used a much more restricted parametrization of duality violations in the $V-A$ channel, with four instead of eight parameters.

It is interesting to compare our results for $C_{6,V-A}$ with an analytical expression that is available at the next-to-leading order [24] (see also ref. [25]):

$$C_{6,V-A} = -\frac{32}{9} \pi \left(1 + \frac{119}{24\pi} \alpha_s(s_0) \right) \alpha_s(s_0) (\rho_1 + \rho_5) \langle \bar{q}q(s_0) \rangle^2 \quad (4.12)$$

$$- \frac{2}{3} \alpha_s^2(s_0) (\tilde{\rho}_1 + \tilde{\rho}_5) \langle \bar{q}q(s_0) \rangle^2 .$$

The parameters $\rho_{1,5}$ and $\tilde{\rho}_{1,5}$ parametrize deviations from the so-called vacuum saturation approximation (VSA), in which they are all normalized to unity. Values for $\rho_{1,5}$ from our fits have already been discussed in Refs. [2, 3]. Numerically, at $s_0 \approx m_\tau^2$ the second line of Eq. (4.12) only contributes about a few percent, so that precise values for $\tilde{\rho}_{1,5}$ are irrelevant. On the other hand, in the VSA the first line of Eq. (4.12) yields

$$C_{6,V-A}^{\text{VSA}} = -4.4 \times 10^{-3} \text{ GeV}^6 , \quad (4.13)$$

where $\langle \bar{q}q(m_\tau^2) \rangle = -(272 \text{ MeV})^3$ [26], together with our result for $\alpha_s(m_\tau^2)$ has been employed. As the next-to-leading order correction in Eq. (4.12) amounts to about 50%, an error of that size should be attributed to the numerical value (4.13). Therefore, the difference between our central fit result of Eqs. (4.11) and (4.12) could either be due to higher-order QCD corrections or a breaking of the VSA. At any rate, no significant deviations from the VSA are observed and the results in Eqs. (4.11) and (4.13) are nicely compatible.

V. CONCLUSION

We used results of earlier fits to the non-strange vector- and axial-channel spectral functions obtained from OPAL hadronic τ decay data in order to estimate the low-energy constant combinations L_{10}^{eff} and C_{87}^{eff} , as well as the operator product coefficients $C_{6,V-A}$ and $C_{8,V-A}$. Our best values are

$$\begin{aligned} L_{10}^{\text{eff}} &= (-6.45 \pm 0.09) \times 10^{-3} , \\ C_{87}^{\text{eff}} &= (8.47 \pm 0.29) \times 10^{-3} \text{ GeV}^{-2} , \\ C_{6,V-A} &= (-6.6 \pm 1.1) \times 10^{-3} \text{ GeV}^6 , \\ C_{8,V-A} &= (5 \pm 5) \times 10^{-3} \text{ GeV}^8 . \end{aligned} \tag{5.1}$$

For a comparison with the values of L_{10}^{eff} and C_{87}^{eff} obtained in Ref. [19], we refer to Sec. IV A. For comparisons with other values for $C_{6,V-A}$ and $C_{8,V-A}$ obtained in the literature, see Fig. 3. As emphasized in Sec. IV C, for $C_{6,V-A}$ and $C_{8,V-A}$ the results are rather sensitive to small variations in the data, and to the details of the fits. In contrast, we expect the results for L_{10}^{eff} and C_{87}^{eff} to be rather robust, since these values are dominated by the low- Q^2 range of the data, where the experimental errors are small. For a comparison of the low- Q^2 behavior of $\Pi_{V-A}(Q^2)$ with ChPT to order p^6 , we refer to Sec. IV B. We find that order- p^8 effects, not included in our chiral fits, are clearly visible in C_{87}^r , but not in L_{10}^r . This is consistent with what one would expect: taking into account order- p^6 terms stabilizes the values of the LECs at lower order.

We demonstrated in both Ref. [3] and Ref. [2], that our fits satisfy both Weinberg sum rules, as well as the DGMLY sum rule for the pion electromagnetic self-energy [27] within errors, though none of these were enforced in the fits. The situation is thus very much analogous to that of the analysis of Refs. [16] and [19]. There, the set of “acceptable” DV parameter combinations was generated by requiring the corresponding DV contributions to the Weinberg and DGMLY sum rules to be such that all three sum rules were satisfied within the experimental errors on the data part of these sum rules, *i.e.*, the integral from 0 to s_0 in Eq. (2.2). On this point, there is thus no relevant difference between the strategies employed in Refs. [2, 3] and Refs. [16, 19].

There are important differences, however. First, Refs. [16, 19] started from an *ansatz* of the form (2.14) for the DV part of $\rho_V - \rho_A$ involving only four parameters rather than four for each of the two channels separately. The possibility that the vector and axial DV contributions are such as to allow the $V - A$ combination to be expressed in this simplified form, however, is not supported by the results of our fits to the individual vector and axial channels. Furthermore, the procedure of Ref. [16], described in more detail in Ref. [28], does not take into account the correlations between the data and DV parameters induced by the use of the Weinberg and DGMLY sum rules. Neither were the correlations between the data and the DV parameters taken into account when using their results to evaluate the quantities of interest, L_{10}^{eff} , *etc.* In our analysis, we have taken these correlations fully into account, and find them to have a significant effect.

Finally, most of the earlier results shown in Fig. 3 are based on ALEPH data [8, 29]. At least for those earlier works which employed the 2005/2008 version of

these data [8], the incompleteness of the 2005/2008 correlation matrices [9] should be born in mind when appraising these results. We wish to reiterate the expectation that inclusive spectral functions extracted from BaBar or Belle would be of great help in reducing the uncertainties on $C_{6,V-A}$ and $C_{8,V-A}$, for the reasons already discussed in Ref. [2].

Acknowledgments

KM thanks the Department of Physics at the Universitat Autònoma de Barcelona for hospitality. DB is supported by the Alexander von Humboldt Foundation, MG is supported in part by the US Department of Energy, and in part by the Spanish Ministerio de Educación, Cultura y Deporte, under program SAB2011-0074. MJ and SP are supported by CICYTFEDER-FPA2008-01430, FPA2011-25948, SGR2009-894, the Spanish Consolider-Ingenio 2010 Program CPAN (CSD2007-00042). KM is supported by a grant from the Natural Sciences and Engineering Research Council of Canada.

-
- [1] K. Akerstaff *et al.* [OPAL Collaboration], Eur. Phys. J. C **7**, 571 (1999) [arXiv:hep-ex/9808019].
 - [2] D. Boito, M. Golterman, M. Jamin, A. Mahdavi, K. Maltman, J. Osborne and S. Peris, Phys. Rev. D **85**, 093015 (2012) [arXiv:1203.3146 [hep-ph]].
 - [3] D. Boito, O. Catà, M. Golterman, M. Jamin, K. Maltman, J. Osborne and S. Peris, Phys. Rev. **D84**, 113006 (2011) [arXiv:1110.1127 [hep-ph]].
 - [4] M. Beneke, D. Boito and M. Jamin, arXiv:1210.8038 [hep-ph].
 - [5] K. Maltman and T. Yavin, Phys. Rev. **D78**, 094020 (2008) [arXiv:0807.0650 [hep-ph]].
 - [6] O. Catà, M. Golterman and S. Peris, JHEP **0508**, 076 (2005) [hep-ph/0506004].
 - [7] O. Catà, M. Golterman and S. Peris, Phys. Rev. **D77**, 093006 (2008) [arXiv:0803.0246 [hep-ph]].
 - [8] S. Schael *et al.* [ALEPH Collaboration], Phys. Rept. **421**, 191 (2005) [arXiv:hep-ex/0506072].
 - [9] D. Boito, O. Catà, M. Golterman, M. Jamin, K. Maltman, J. Osborne and S. Peris, arXiv:1011.4426 [hep-ph].
 - [10] S. Weinberg, Phys. Rev. Lett. **18**, 507 (1967).
 - [11] E. G. Floratos, S. Narison and E. de Rafael, Nucl. Phys. B **155**, 115 (1979).
 - [12] K. G. Chetyrkin, V. P. Spiridonov and S. G. Gorishnii, Phys. Lett. **B160**, 149 (1985).
 - [13] M. Davier, L. Girlanda, A. Höcker and J. Stern, Phys. Rev. D **58**, 096014 (1998) [hep-ph/9802447].
 - [14] G. Amorós, J. Bijnens and P. Talavera, Nucl. Phys. B **568**, 319 (2000) [hep-ph/9907264].
 - [15] M. González-Alonso, A. Pich and J. Prades, Phys. Rev. D **78**, 116012 (2008) [arXiv:0810.0760 [hep-ph]].
 - [16] M. González-Alonso, A. Pich and J. Prades, Phys. Rev. **D81**, 074007 (2010) [arXiv:1001.2269 [hep-ph]].

- [17] B. Blok, M. A. Shifman and D. X. Zhang, Phys. Rev. D **57**, 2691 (1998) [Erratum-ibid. D **59**, 019901 (1999)] [arXiv:hep-ph/9709333]; I. I. Y. Bigi, M. A. Shifman, N. Uraltsev and A. I. Vainshtein, Phys. Rev. **D59**, 054011 (1999) [hep-ph/9805241]; M. A. Shifman, [hep-ph/0009131]; M. Golterman, S. Peris, B. Phily and E. de Rafael, JHEP **0201**, 024 (2002) [hep-ph/0112042].
- [18] A. A. Pivovarov, Z. Phys. C **53**, 461 (1992) [Sov. J. Nucl. Phys. **54**, 676 (1991)] [Yad. Fiz. **54** (1991) 1114] [arXiv:hep-ph/0302003]; F. Le Diberder and A. Pich, Phys. Lett. **B286**, 147 (1992).
- [19] M. González-Alonso, A. Pich and J. Prades, Phys. Rev. D **82**, 014019 (2010) [arXiv:1004.4987 [hep-ph]].
- [20] O. Catà, M. Golterman and S. Peris, Phys. Rev. **D79**, 053002 (2009) [arXiv:0812.2285 [hep-ph]].
- [21] A. A. Almasy, K. Schilcher and H. Spiesberger, Eur. Phys. J. C **55**, 237 (2008) [arXiv:0802.0980 [hep-ph]]; P. Masjuan and S. Peris, JHEP **0705**, 040 (2007) [arXiv:0704.1247 [hep-ph]]; C. A. Dominguez and K. Schilcher, Phys. Lett. B **581**, 193 (2004) [hep-ph/0309285]; S. Narison, Phys. Lett. B **624**, 223 (2005) [hep-ph/0412152]; K. N. Zyablyuk, Eur. Phys. J. C **38**, 215 (2004) [hep-ph/0404230]; S. Friot, D. Greynat and E. de Rafael, JHEP **0410**, 043 (2004) [hep-ph/0408281]; J. Rojo and J. I. Latorre, JHEP **0401**, 055 (2004) [hep-ph/0401047]; V. Cirigliano, J. F. Donoghue, E. Golowich and K. Maltman, Phys. Lett. B **555**, 71 (2003) [hep-ph/0211420]; J. Bijnens, E. Gamiz and J. Prades, JHEP **0110**, 009 (2001) [hep-ph/0108240].
- [22] V. Cirigliano, E. Golowich and K. Maltman, Phys. Rev. D **68**, 054013 (2003) [hep-ph/0305118].
- [23] J. Bijnens and P. Talavera, JHEP **0203**, 046 (2002) [hep-ph/0203049].
- [24] L. V. Lanin, V. P. Spiridonov and K. G. Chetyrkin, Sov. J. Nucl. Phys. **44**, 892 (1986).
- [25] E. Braaten, S. Narison and A. Pich, Nucl. Phys. B **373**, 581 (1992).
- [26] M. Beneke and M. Jamin, JHEP **0809**, 044 (2008) [arXiv:0806.3156 [hep-ph]].
- [27] T. Das, G. S. Guralnik, V. S. Mathur, F. E. Low and J. E. Young, Phys. Rev. Lett. **18**, 759 (1967).
- [28] M. González-Alonso, Ph.D. thesis (2010).
- [29] R. Barate *et al.* [ALEPH Collaboration], Eur. Phys. J. **C4**, 409 (1998).